Publications of the Astronomical Society of Australia (2025), 42, e065, 7 pages
doi:10.1017/pasa.2025.10034

Research Article

Can old sleepy galaxies have huge black holes in them without dark matter?

Eappen and Kroupa wrote this!

In a nutshell:

Can a new model explain how huge black holes form in 'dead' galaxies? This paper tests what conditions are needed for that to happen under the model. They also compare it to well-known patterns, like the link between mass and velocity, which come from real observations. The model matches these observations without needing dark matter. It also shows that how gas behaves when a galaxy first forms plays a big role in creating these giant black holes.

Keywords: Galaxy: evolution; galaxy: formation; galaxies: elliptical and lenticular; cD; Galaxies: fundamental parameters; black holes

(Received 8 December 2024; revised 21 April 2025; accepted 11 May 2025)

Background:

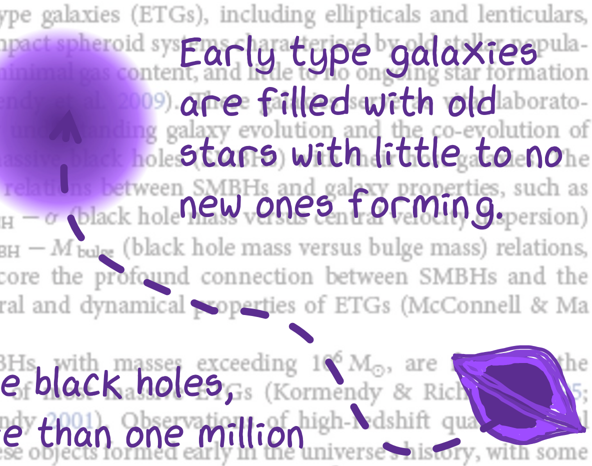

Early type galaxies are filled with old stars with little to no new ones forming.

Huge black holes, more than one million times the mass of the sun, have been found in early type galaxies. These are thought to have formed really early in cosmic history!

How do huge black holes form? One option is through interactions in dense stellar environments. Maybe two smaller black holes merge!

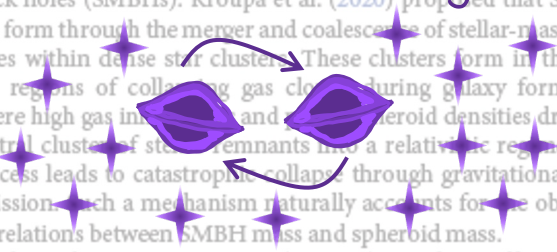

One theory changes how gravity behaves at low accelerations, explaining some observations without dark matter. In some cases, it matches or even outperforms the standard cosmological model. If correct, it could reshape our understanding of galaxy and black hole evolution.

Corresponding author: Robin Eappen, Email: robin.eappen@gmail.com.
Cite this article: Eappen R and Kroupa P. (2025) Growth of black holes at the centre of early-type galaxies in MOND. Publications of the Astronomical Society of Australia 42, e065, 1–7. https://doi.org/10.1017/pasa.2025.10034

The biggest black holes are also called supermassive black holes!

the dynamical friction test further questions their existence (Oehm & Kroupa 2024). Within MOND, ETGs are thought to form via the monolithic collapse of primordial pre-galactic gas clouds, producing high stellar densities and rapid star formation (Eappen et al. 2022). Stellar-mass black holes forming in dense central clusters d[illegible] and coalesce to create SMBHs, as suggested by Kroupa et al. (2020).

Supermassive black hole properties have been linked to the motions at the center of the galaxy.

[illegible] of RAMSES (PoR) code (Lüghausen, Famaey, & Kroupa 2015; Nagesh et al. 2021) have reproduced many properties of observed galaxies, including the emergence of the downsizing trend in ETGs (Eappen et al. 2022). These simulations provide a platform for studying the formation and evolution of ETGs under MOND and their potential to host SMBHs. However, while the downsizing relations and star formation histories of ETGs in MOND have been explored, the role of the central gravitational potential ($\Phi_{central}$) – a key determinant of SMBH formation – remains und[illegible] strongly correlate with central galaxy dynamics, linking $\Phi_{central}$ to velocity dispersion, gas inflow, and scaling relations such as the $M_{BH} - \sigma$ relation (McConnell & Ma 2013).

To test if supermassive black holes could form in early-type galaxies under the MOND model, they check whether the central density is linked to how much gas flows in and how varied the velocities are. (this is introducing the method!)

In this study, we investigate $\Phi_{central}$ and gas inflow rates in ET[illegible] PoR code. We aim to determine whether these systems create the necessary con[illegible] SMBH masses are consistent with the observed $M_{BH} - \sigma$ scaling relation. To achieve this, we analyse the evolution of the central gravitational potential and gas inflow rates during the early phases of galaxy formation. Additionally, based on the work of Kroupa et al. (2020), we evaluate SMBH masses by assuming that a fraction of the central stellar mass collapses into the SMBH. Finally, we compare the simulated SMBH masses to observed scaling relations to assess whether MOND-modelled ETGs can host SMBHs consistent with empirical data. This work builds on the foundation of Eappen et al. (2022) and aims to connect the dynamics of MOND-modelled ETGs with SMBH formation, providing new insights into galaxy evolution in alternative gravity frameworks.

Methods – How they modelled:

In this study, we use the model galaxies formed with an initial post-Big-Bang gas cloud radius ($R_{initial}$) of 500 kpc as presented in Eappen et al. (2022). Here, we specifically focus on analysing $\Phi_{central}$, gas inflow rates, and estimating the potential mass of a SMBH that could form within the galaxy. For these analyses, we [illegible] lution compared to other models. This decision is motivated by the [illegible] evolution during the critical phases of galaxy formation. However, due to computational limitations, we have [illegible] our analysis to this single high temporal resolution model. [illegible] tial mass reservoir [illegible] for SMBH formation, we use the gas mass evolution data from our [illegible] (e38), which employs an initial cloud radius [illegible] kpc. Although we mention multiple models with this initial radius (e35, e36, e37, e38 and e39 from Table 1 of Eappen et al. 2022), our SMBH mass estimate is based specifically on the e38 model. The time reported here is relative to the start of the simulation. The simulation box has a side length of 1 Mpc, providing a sufficient volume to follow the collapse and evolution of the isolated galaxy model. Throughout the analysis, we define the 'central region' based on the centre of

They model galaxies that start from a gas cloud about 1000 times the size of our milky way. Specifics given in Eappen's 2022 paper!

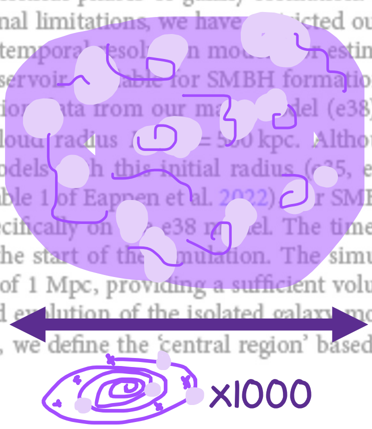

mass of the stellar particles within a 500 kpc radius. This approach ensures that the centre is dynamically tracked throughout the simulation, independent of any fixed box coordinates.

The simulations are further constrained by a maximum spatial resolution of 0.24 kpc (which is the physical size of an individual grid cell at the highest level of refinement. However, we note that accurately resolving potential gradients typically requires several grid cells. Thus, the effective resolution of our simulation is somewhat larger than the cell size, approximately ≈1 kpc in the [illegible] refinement (AMR) capabilities of the PoR code. Improving the spatial resolu[illegible] infeasible due to the significant computational cost associated with higher resolution MOND simulations. While the PoR code in QUMOND mode – the quasi-linear formulation of MOND (Milgrom 2010) in which the modified gravitational field is derived via a two-step Poisson solver indeed requires at most twice the computational time compared to Newtonian [illegible] primary limitation for increasing refinement levels in our simulation was the available memory capacity. Higher refinement would substantially increase memory requirements due to the number of cells and particles, and future work will aim to address this with improved computational resources. Despite these limitations, the model allows us to explore key aspects of SMBH formation and galaxy evolution within the framework of MOND. A detailed description of the model formation process, including the initial conditions and simulation setup, can be found in Eappen et al. (2022).

They talk about what simulation sizes are computationally feasible.

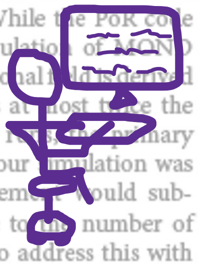

Gravitational Potential Equations

The gravitational potential at the centre of the model, $\Phi_{central}$, is calculated in the simulation by solving the MOND-modified Poisson equation. In MOND, the gravitational potential Φ is governed by the equation:

Gravitational potential tells us how hard gravity is pulling at a certain place, and how much energy it would take to get there or escape from it.

$$\Delta\Phi = 4\pi G \rho_b \ldots \nabla\left[\tilde{\nu}\left(\frac{|\nabla\phi|}{a_0}\right)\nabla\phi\right] \quad (1)$$

where $\Delta\Phi$ is the Laplacian of the gravitational potential, ρ_b is the baryonic matter density, G is the gravitational constant, a_0 is the MOND acceleration constant, ϕ is the Newtonian potential, and $\tilde{\nu}(y)$ is the MOND transition function, with $y = |\phi|/a_0$. The equation represents the [illegible] in the QUMOND framework, as implemented in the PoR code. This equation modifies Newtonian gravity at low accelerations ($g < a_0$) by introducing non-linearity in the relationship between mass and potential. The PoR code numerically solves this equation [illegible] galaxy.

To figure out the gravitational pull in a certain area, the first step is to see how much normal matter is packed into that space. This is called baryonic density — "baryonic" just means ordinary stuff like stars, planets, and even people, all made of protons and neutrons.

[illegible] the baryonic density distribution (ρ_b), which represents the distribution of gas and stars in the galaxy. Using this density, the Newtonian Poisson equation, is first solved to calculate the Newtonian potential $\phi(r)$:

$$\Delta\phi = 4\pi G \rho_b. \quad (2)$$

From the Newtonian potential, the code computes the phantom dark matter density (ρ_{ph}) that arises due to the MOND modification. This density is given by:

We also need to know how much phantom matter we would need under a Newtonian physics model.

$$\rho_{ph} = \frac{1}{4\pi G}\nabla\left[\tilde{\nu}\left(\frac{|\nabla\phi|}{a_0}\right)\nabla\phi\right] \quad (3)$$

https://doi.org/10.1017/pasa.2025.10034 Published online by Cambridge University Press

The total gravitational potential Φ is then recalculated by solving the Poisson equation, which incorporates both ρ_b and ρ_{ph}:

Gravitational potential ∝ density of real matter and phantom matter.

$$\Delta\Phi = 4\pi G(\rho_b + \rho_{ph}). \quad (4)$$

$\Phi_{central}$ is extracted from the simulation output at specific radii, such as 1, 0.8, and 0.6 kpc, at each time step (The simulation outputs are saved at intervals of 10 Myr, allowing us to follow the evolution of inflow rates and dynamical changes over time. For the period of rapid collapse (≈3–5 Gyr), this corresponds to a temporal resolution of 100 snapshots per Gyr). This value represents the depth of the gravitational potential well at the galaxy's centre and evolves as the galaxy forms and stabilises.

Little gravitational potential:

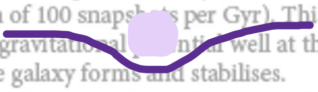

Physically, $\Phi_{central}$ reflects the gravitational strength in the galaxy's core. A deeper potential well corresponds to a denser and more massive central region. The evolution of $\Phi_{central}$ over time provides insight into the baryonic collapse and the formation of a dense core, processes that are critical for driving gas inflows and forming a SMBH. Additionally, the differences in $\Phi_{central}$ at various radii, such as between 1 and 0.6 kpc, reveal the steepness of the potential gradient, which influences the dynamics of gas inflows and central star formation.

Big gravitational potential:

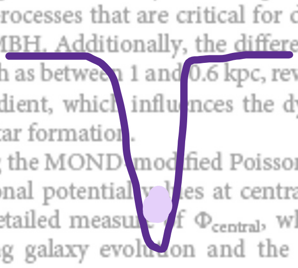

By solving the MOND-modified Poisson equation and extracting gravitational potential values at central radii, the simulation provides a detailed measure of $\Phi_{central}$, which is fundamental to understanding galaxy evolution and the conditions for SMBH formation in MOND.

How to calculate how much gas falls to the centre?

2.3 Gas inflow to the centre of the model galaxies [illegible]

The gas inflow rates at different radii ($r = 1$ kpc, 0.8 kpc, 0.6 kpc) were computed using data from the simulation. The inflow rate ($\dot{M}_{gas}$) was calculated as the rate of change of gas mass (M_{gas}) within a given radius over a discrete time interval. For each radius, the inflow rate is given by:

How much gas is falling into the centre can be calculated at each radius and timestep. It is equal to how much mass has been gained or lost over what timeframe at that point in space.

$$\dot{M}_{gas}(r,t) = \frac{\Delta M_{gas}(r,t)}{\Delta t}, \quad (5)$$

where $\dot{M}_{gas}(r,t)$ is the inflow rate at radius r and time t, $\Delta M_{gas}(r,t)$ [illegible] is the change in gas mass within radius r between consecutive time snapshots, Δt is the time interval between these snapshots. The gas mass is calculated by summing the contributions from individual cells within the specified radius. For each cell, the gas mass is obtained by multiplying the cell volume by its gas density. Cells whose centres lie within the selected radius are included in full. Since the AMR grid structure results in varying cell resolutions, this calculation automatically accounts for local resolution differences. We note that we do not perform partial cell volume calculations for boundary cells; cells are either fully included or excluded based on their centre position.

The simulation data provides $M_{gas}(r,t)$ for discrete time points. Using the differences between consecutive snapshots, the inflow rate is computed for the midpoints of these time intervals to align with the calculated rates.

How to calculate the black hole mass?

~theoretically~

2.4 Black hole mass estimation [illegible]

This analysis estimates the black hole mass (M_{BH}) as a fraction of the central stellar mass and computes the central velocity dispersion (σ) for galaxies within the simulation. The results are compared to the observed $M_{BH} - \sigma$ scaling relation from McConnell & Ma (2013).

$$r = \sqrt{x^2 + y^2 + z^2}$$

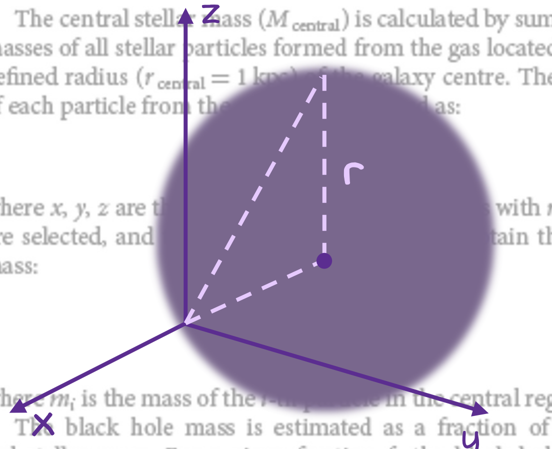

The central stellar mass ($M_{central}$) is calculated by summing the masses of all stellar particles formed from the gas located within a defined radius ($r_{central} = 1$ kpc) of the galaxy centre. The distance of each particle from the [illegible] as:

(6)

where x, y, z are t[illegible] with $r \leq r_{central}$ are selected, and [illegible]tain the central mass:

(7)

where m_i is the mass of the i-th particle in the central region.

The black hole mass is estimated as a fraction of the central stellar mass. For a given fraction f, the black hole mass is given by:

Black hole mass ∝ Central star Mass

$$M_{BH} = f \times M_{central}. \quad (8)$$

Fractions ranging from $f = 0.1$ to $f = 1.0$ are used to explore the contribution of the central stellar mass to the SMBH. These fractions are realistic (Kroupa et al. 2020) as the stellar initial mass function (IMF) depends on the metallicity and [illegible] on the star-forming gas and is top-heavy under the relevant physical conditions such that the majority of the cluster's mass ends up being in stellar-mass black holes (Marks et al. 2012; Jeřábková et al. 2018; Kroupa et al. 2020; Kroupa et al. 2024).

How dependent blackhole mass is on star mass relies on initial mass function assumption and how metallic the gas is assumed to be.

The 3D central velocity dispersion (σ_{total}) is calculated using the particle velocities in the central region. For each velocity component (v_x, v_y, v_z), the dispersion is computed as:

$$\sigma_x = \sqrt{\frac{1}{N}\sum_{i=1}^{N}(v_{x,i} - \bar{v}_x)^2}, \quad (9)$$

where N is the number of particles, $v_{x,i}$ is the velocity of the i-th particle, and $\bar{v}_x$ is the mean velocity in the x-direction. Similar expressions are used for σ_y and σ_z. The total 3D central velocity dispersion is:

Velocity dispersion in a direction measures how much the measurement differs from the average velocity.

$$\sigma_{total} = \sqrt{\sigma_x^2 + \sigma_y^2 + \sigma_z^2}. \quad (10)$$

The black hole masses and the computed velocity dispersion values are compared to the observed $M_{BH} - \sigma$ relation from McConnell & Ma (2013):

Black hole mass as a function of velocity dispersion formula.

$$\log_{10}(M_{BH}) = 8.39 + 5.20 \cdot \log_{10}\left(\frac{\sigma}{200}\right), \quad (11)$$

where σ is in km/s. This comparison provides insight into whether the simulated galaxies reproduce the observed scaling relation between black hole mass and central velocity dispersion, thereby validating the model's predictions for SMBH formation.

Results!

Is the gravitational potential well deep enough for stuff to not escape?

3.1 The gravitational potential well at the centre: the formation of a SMBH?

We analyse the evolution of the gravitational potential difference at the centre of our model ETG (e38), which forms a total stellar mass of 0.6×10^{11} $M_\odot$. Fig. 1 shows the evolution of the relative gravitational potential difference relative to the potential

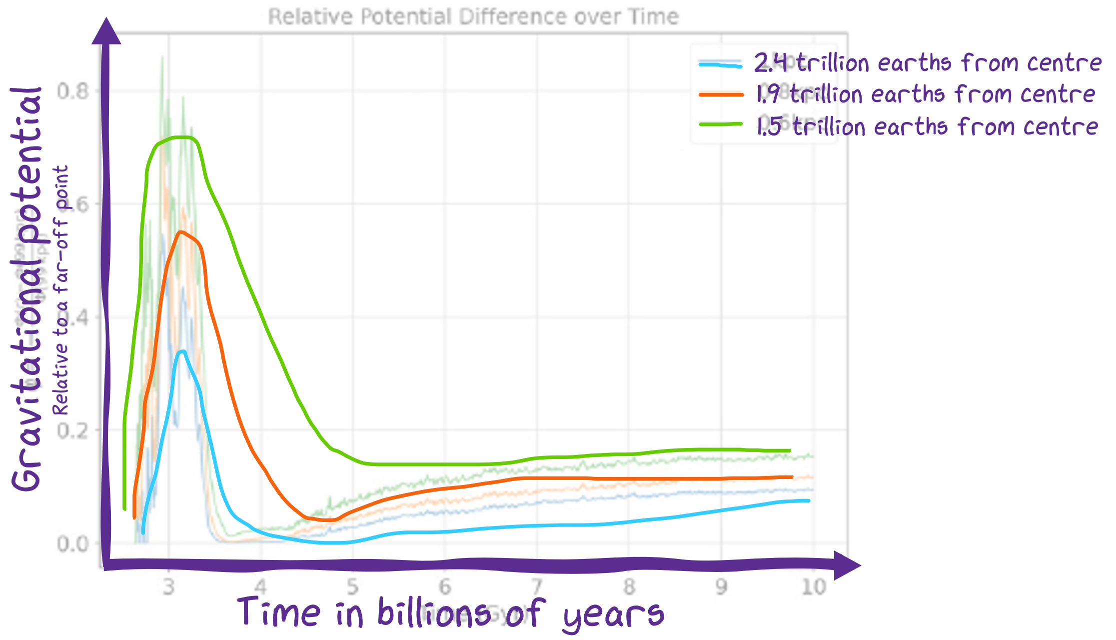

Figure 1. Time evolution of the relative gravitational potential difference between the central region (at radii of 1, 0.8, and 0.6 kpc) and a reference point at 99 kpc. The potential deepens rapidly during the collapse phase (≈ 3–5 Gyr), stabilising thereafter. The use of potential difference avoids dependence on absolute values and reflects the physical depth of the potential well relative to the galaxy outskirts.

at a radius of 99 kpc between three central radii (1 kpc, 0.8 kpc, and 0.6 kpc) over 10 Gyr.

The reference radius at 99 kpc corresponds to the outskirts of our simulated system, providing a consistent frame of reference for measuring the depth of the central potential well. While an ideal reference would be at infinity, the finite simulation volume necessitates this practical choice. The potential difference highlights the deepening of the gravitational well relative to the galaxy outskirts.

Within the first 5 billion years the gravitational well rapidly gets deeper, allowing mass to fall, particularly when closer to the centre. These are ingredients to create Black holes!

During the initial 4.5 Gyr, the relative potential difference increases sharply, coinciding with the collapse of baryonic gas and the [illegible]. This [illegible] reflects the rapid deepening of the central gravitational well, driven by gas [illegible]. This phase is critical as it establishes the gravitational environment that facilitates further mass inflow toward the galactic centre.

Beyond 5 Gyr, the potential difference stabilises, indicating that the system transitions to a more dynamically settled state. Notably, the deepest potential difference is seen at smaller radii (0.6 kpc), emphasising the concentration of baryonic mass toward the centre and suggesting that any gas reaching these inner regions could contribute to black hole growth.

To assess the role of MOND dynamics in the evolution of the central potential, we computed the acceleration profile at $t = 4.4$ Gyr, corresponding to the peak of baryonic collapse (Fig. 2). The accelerations within the inner ≈ [illegible] kpc exceed the MOND acceleration scale a_0, indicating that the dynamics in the central potential [illegible] Newtonian due to the high baryonic density. MOND effects become significant at larger radii (≈ 8 kpc and [illegible]), potentially aiding the gravitational collapse and mass transport toward the centre.

Dynamics within the well are too fast to be part of the MOND model, MOND is more likely seen at larger radii to help transport mass to the centre.

A comparable observational example is the compact ETG NGC 1277 in the Perseus Cluster, with a total stellar mass of 1.2×10^{11} $M_\odot$ and an effective radius of approximately 1.2 kpc. This galaxy hosts a SMBH with a mass of $\approx 1.7 \times 10^{10}$ $M_\odot$, accounting for nearly 14% of its total stellar mass – far above typical scaling relations. The gravitational potential difference in NGC 1277 is similarly deep, driven by its compact stellar core and massive black hole (Trujillo et al. [illegible] van den Bosch et al. 2012; Yldrm et al. 2017; Ferré-M[illegible] is comparable to the potential differen[illegible] after ≈ 5 Gyr, supporting the noti[illegible] naturally develop deep gravitation[illegible]

These values compare well to NGC 1277

I'm a real picture!

This compa[illegible]nal environment in our simulate[illegible]served properties of real compact [illegible] central potential in both cases und[illegible] cores in establishing conditions [illegible]ation and growth. The evolution of the po[illegible] in our model further supports the idea that compact ETGs can host over-massive SMBHs as a consequence of their early, rapid formation and subsequent stabilisation.

Does enough gas fall into the centre to make a supermassive black hole?

3.2 [illegible]

The gas inflow rates at the same radii (1, 0.8, and 0.6 kpc) are illustrated in Fig. 3 for the critical epoch between 4 and 6 Gyr, corresponding to the period of most rapid potential evolution. At a radius of 1 kpc, gas inflow peaks at rates exceeding 2×10^{10} [illegible] while smaller radii exhibit similarly high but slightly delayed peaks. These inflows correspond to periods of rapid cooling and contraction of gas toward the centre. The sustained high inflow rate over about half a Gyr suggests that sufficient mass can [illegible] central SMBH. Notably, around $t \approx 4.7$ Gyr, the central regions experience an outflow phase, as shown in Fig. 3, driven by feedback mechanisms inherent to the model (Eappen et al. 2022), leading to gas heating and temporary disruption of inflows. After 5 Gyr,

Tldr: Yes!

There is also an outflow phase!

https://doi.org/10.1017/pasa.2025.10034 Published online by Cambridge University Press

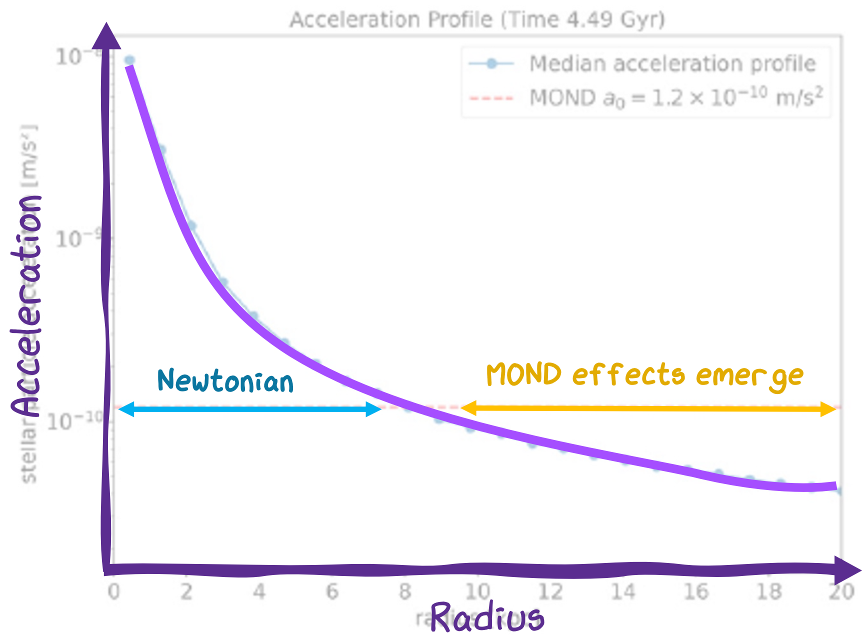

Figure 2. Radial profile of the median stellar particle acceleration at $t = 4.49$ Gyr. The red dashed line indicates the MOND acceleration scale $a_0 = 1.2 \times 10^{-10}$ m/s² ≈ 3.8 pc/Myr². Accelerations in the inner ≈3–4 kpc exceed a_0, indicating that the central region is in the Newtonian regime. MOND effects emerge at larger radii (≈8 kpc), influencing the global gravitational collapse.

outflow rates decline and stabilise, consistent with the exhaustion of central gas reservoirs. This reduction implies that star formation and black hole accretion activity slow significantly, transitioning the system into a quiescent phase.

There is a lot of interesting activity in early time after collapse, how relevant this is to black hole growth requires better resolution simulations.

These findings underscore the importance of the early epochs (4–5 Gyr, [illegible] Gyr after start of collapse, see Fig. 1) as a critical window for black hole growth, during which high inflow rates enable [illegible]. We note that during the time ≈ 3.7 - 4.7 Gyr there is a slowly rising infall rate from 0.1 × [illegible] M⊙/Gyr to 1.1 × [illegible] M⊙/Gyr. The inflow rates exhibit substantial variability after about 4.5 Gyr with fluctuations between strong inflow and outflow on timescales comparable to our snapshot interval driving supernova activity. Given the limited spatial and temporal resolution of our simulation, and the inherent variability in the gas inflow rates, our conclusions regarding the viability of SMBH seed formation remain qualitative. Higher resolution simulations would be required to fully resolve the detailed inflow behaviour at sub-kpc scales relevant for SMBH feeding.

The trends observed in our model align closely with theoretical predictions and observations of ETGs in the literature. For instance, Kroupa et al. (2020) proposed that SMBHs form through the coalescence of stellar-mass black holes in dense star clusters.

Trends align with theory and observation that Kroupa has studied in the past!

These [illegible] systems, rely on significant gas inflows to maintain their density and fuel black hole [illegible] peaking above 2×10^{10} M⊙/Gyr at 1 kpc, provide the necessary conditions for this process, allowing central gas densities to remain high enough to support the formation of the massive clusters. Furthermore, the slight delay in peak inflows at smaller radii (e.g. 0.6 kpc) highlights the gradual inward transport of gas, a feature consistent with the cooling flows observed in present day dense early environments.

Observational studies of high-redshift quasars (e.g. Venemans et al. 2013) have revealed black holes with masses exceeding 10^9 M⊙ by $z \approx 6$, implying efficient accretion mechanisms in the first billion years. This comparison reinforces the notion that the early, gas-rich environment in our simulated ETG is consistent with the conditions required for forming and growing central SMBHs observed in compact ETGs and high-redshift quasars.

Do we see the relationship between the size of the supermassive black hole and the spread of velocities?

3.3 Would the $M_{BH} - \sigma$ scaling relation emerge?

The relationship between M_{BH} and σ is explored in the context of [illegible] of the central stellar mass within 1, 0.8, and 0.6 kpc contributes to black hole formation. This is based on the model of Kroupa et al. (2020) in which [illegible] of the forming spheroidal galaxy, each 10 Myr. The calculated black hole [illegible] of the central stellar mass, are plotted alongside the observed $M_{BH} - \sigma$ relation [illegible] Fig. 4 include the models [illegible] Eappen et al. (2022) as well as the observed ETGs from McConnell & Ma (2013) and [illegible].

Black holes with less central star mass contribution and larger velocity spread give the best agreement to the studied relationship.

Black hole masses derived from lower contributions of the central stellar mass (10–50%) and at larger central velocity dispersion exhibit good agreement with the observed $M_{BH} - \sigma$ relation [illegible] central stellar mass contributes to the black hole's formation, then the resulting masses are consistent with those observed in real ETGs. This indicates that a minimum threshold of stellar mass contribution is necessary to match observed SMBH properties [illegible] et al. (2020). We acknowledge that the spatial scales considered in our analysis [illegible] the physical scales relevant for SMBH accretion, which are typically in the parsec range. Therefore, our estimates represent upper limits to the mass reservoir potentially available for SMBH formation, and the actual mass feeding the black hole would likely be orders of magnitude smaller.

Therefore there must be a minimum stellar mass contribution threshold.

However they can only see an upper limit of mass available with the resolution used.

https://doi.org/10.1017/pasa.2025.10034 Published online by Cambridge University Press

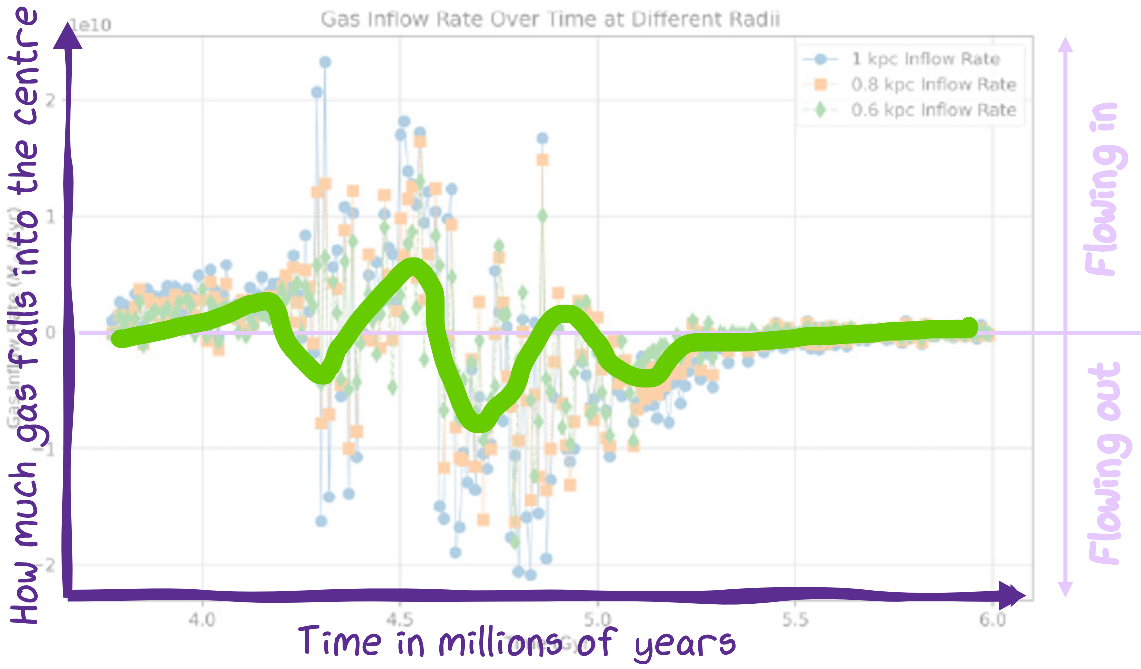

Figure 3. Gas inflow rate over time at different radii (1, 0.8, and 0.6 kpc). The plot illustrates fluctuations in the inflow rate of gas (in $M_\odot$/Gyr) during the time range from 4 to 6 Gyr. Significant variability is observed, particularly in the interval between 4.0 and 5.0 Gyr, with notable peaks and troughs, indicative of dynamic processes affecting gas inflow at these radii.

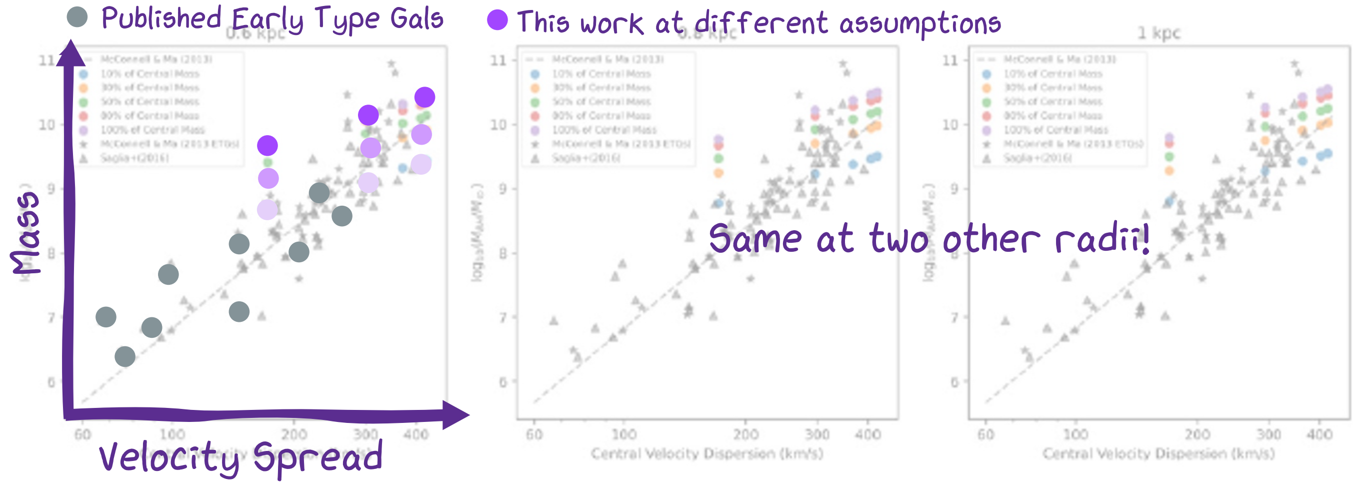

Figure 4. The calculated black hole masses for the model relics (e35, e36, e37, e38 and e39) from Eappen et al. (2022), based on 10%, 30%, 50%, 80%, and 100% of the central stellar mass, are plotted alongside the observed $M_{BH} - \sigma$ relation from McConnell & Ma (2013). The plotted black stars and black triangles are the ETGs from McConnell & Ma (2013) and Saglia et al. (2016) respectively.

The analysis highlights the capability of MOND dynamics to support the formation of SMBHs in ETGs formed via monolithic collapse. The rapid deepening of the central gravitational potential during the first 0.5 Gyr after begin of the collapse, coupled with high gas inflow rates, creates a conducive environment for black hole seeding and growth.

Quick take away messages:

Conclusion

In this study, we investigated the evolution of ETGs within a MOND framework, focusing on the central gravitational potential, gas inflow rates, and the relationship between black hole mass and central velocity dispersion. Using simulations, we analysed the gravitational and dynamical properties of a model galaxy with a total stellar mass of 0.6×10^{11} $M_\odot$, providing insights into the mechanisms governing the formation and growth of SMBHs in compact systems.

- Gravitational potential decreases severely very quickly after the collapse of matter

The evolution of the central gravitational potential reveals a sharp decline during the first 0.5 Gyr after the start of the collapse, corresponding to the rapid collapse of baryonic matter and the formation of the stellar population. This phase is marked by the deepening of the central potential well. The deeper gravitational potential at smaller radii (e.g. 0.6 kpc) underscores the concentration of baryonic [illegible] necessary for sustained gas inflows and SMBH formation.

- Deep potential wells close to the centre confirm conditions for gas inflows and properties for the formation of huge black holes.

Gas inflow rates during the critical epoch between [illegible] and 1.5 Gyr after the collapse starts exhibit peaks exceeding $2 \times 10^{[illegible]}$ $M_\odot$/Gyr at 1 kpc, with similarly high but slightly delayed peaks at 0.8 and 0.6 kpc. The subsequent outflow rates and their decline rates after 4.7 Gyr reflects stellar activity and the depletion

https://doi.org/10.1017/pasa.2025.10034 Published online by Cambridge University Press

of gas reservoir, transitioning the system into a quiescent phase. Variations in the adopted feedback prescriptions could significantly influence the inflow dynamics and star formation rates, potentially altering the efficiency of central mass accumulation. Exploring these effects will be the subject of future work. This early period of high inflow rates is crucial for fuelling the growth of the central SMBH and forming a dense stellar core, consistent with the analytical results by Kroupa et al. (2020).

Finally, the relationship between $M_{\rm BH}$ and σ was examined by assuming various fractions (10%, 30%, 50%, 80%, and 100%) of the central stellar mass contribute to the black hole. Black hole masses derived from this align closely with the observed $M_{\rm BH} - \sigma$ [illegible] dispersions (σ > 200 km/s). The results suggest that the combination of a deep gra[illegible] rates, and significant central mass contributions is essential for forming SMBHs consistent with those observed in real galaxies. A more accurate estimate of the SMBH formation potential would require resolving sub-pa[illegible] accretion physics. While our current resolution limits such analysis, the observed collapse an[illegible] framework for assessing early SMBH formation in MOND.

- Early type galaxies made within MOND model work with observed relationships.
- Early gas inflows and gravitational potential evolution is super important to growing big black holes!

Overall, our findings demonstrate that ETGs formed within the MOND framework have the potential to naturally reproduce many of the observed properties of ETGs, including their dense cores, quiescent phases, and the $M_{\rm BH} - \sigma$ relation. These results underscore the importance of early gas inflows and gravitational potential evolution in shaping the growth of SMBHs and the structural properties of ETGs, offering a viable pathway for understan[illegible].

- The simulations had resolution restraints.

However, we recognise certain limitations in this work. The radii typically around 0.1 kpc or smaller, are not fully resolved in our simulations due to computational limitations. As a result, the work presented here provides only a basic estimate of the conditions for SMBH formation and growth in MOND. This is a simplified approach that does not account for complex processes such as detailed feedback mechanisms, the actual coalescence of the cluster of stellar remnants to a SMBH seed, relativistic effects, or accretion dynamics at smaller scales. Nonetheless, this work offers a foundational framework for future MOND cosmological simulations, highlighting the importance of early gas inflows and gravitational potential evolution in shaping compact ETGs and their central SMBHs. Future efforts to incorporate finer resolutions and additional physics into MOND-based simulations will be critical for achieving a more comprehensive understanding of these processes.

- They left some stuff out.
- Lots more work to do!

Acknowledgement. The author R.E would like to thank KFPP for their support. We thank the DAAD Bonn–[illegible] European Exchange programme at the University of Bonn and Prague for support.

Thanks!

Data Availability. None.

Where did all these ideas come from?:

References

Banik, I., & Zhao, H. 2022, Symmetry, 14, 1331. https://doi.org/10.3390/sym14071331. arXiv: 2110.06936 [astro-ph.CO].

Eappen, R., Kroupa, P., Wittenburg, N., Haslbauer, M., & Famaey, B. 2022, MNRAS, 516, 1081. https://doi.org/10.1093/mnras/stac2229. arXiv: 2209.00024 [astro-ph.GA].

Faber, S. M., & Gallagher, J. S. 1979, ARA&A, 17, 135. https://doi.org/10.1146/annurev.aa.17.090179.001031.

Fan, X., et al. 2003, AJ, 125, 1649. https://doi.org/10.1086/368246. arXiv: astro-ph/0301135 [astro-ph].

Ferré-Mateu, A., Trujillo, I., Martn-Navarro, I., Vazdekis, A., Mezcua, M., Balcells, M., & Domnguez, L. 2017, MNRAS, 467, 1929. [illegible] [astro-ph.GA].

Jerábková, T., Hasani Zonoozi, A., Kroupa, P., Beccari, G., Yan, Z., [illegible] & Zhang, [illegible] 2018, A&A, 620, A39. https://doi.org/10.1051/0004-6361/201833055. arXiv: 1809.04603 [astro-ph.GA].

Kormendy, J. 2001, in Revista mexicana de astronomia y astrofisica conference series, Revista Mexicana de Astronomia y Astrofisica Conference Series, ed. J. Cantó, & L. F. Rodrguez, 10, 69.

Kormendy, J., Fisher, D. B., Cornell, M. E., & Bender, R. 2009, ApJS, 182, 216. https://doi.org/10.1088/0067-0049/182/1/216. arXiv: 0810.1681 [astro-ph].

Kormendy, J., & Richstone, D. 1995, ARA&A, 33, 581. https://doi.org/10.1146/annurev.aa.33.090195.003053.

Kroupa, P., Gjergo, E., Jerabkova, T., & Yan, Z. 2024, 2410.07311

Kroupa, P., Subr, L., Jerabkova, T., & Wang, L. 2020, MNRAS, 498, 5652. https://doi.org/10.1093/mnras/staa2276. arXiv: 2007.14402 [astro-ph.GA].

Lelli, F., McGaugh, S. S., Schombert, J. M., & Pawlowski, M. S. 2017, ApJ, 836, 152. https://doi.org/10.3847/1538-4357/836/2/152. arXiv: 1610.08981 [astro-ph.GA].

Liu, Y., et al. 2016, ApJ, 818, 179. https://doi.org/10.3847/0004-637X/818/2/179. arXiv: 1512.00253 [astro-ph.GA].

Lüghausen, F., Famaey, B., & Kroupa, P. 2015, CJPh, 93, 232. https://doi.org/10.1139/cjp-2014-0168. arXiv: 1405.5963 [astro-ph.GA].

Marks, M., Kroupa, P., Dabringhausen, J., & Pawlowski, M. S. 2012, MNRAS, 422, 2246. https://doi.org/10.1111/j.1365-2966.2012.20767.x. arXiv: 1202.4755 [astro-ph.GA].

McConnell, N. J., & Ma, C.-P. 2013, ApJ, 764, 184. https://doi.org/10.1088/0004-637X/764/2/184. arXiv: 1211.2816 [astro-ph.CO].

McDermid, R. M., et al. 2015, MNRAS, 448, 3484. https://doi.org/10.1093/mnras/stv105. arXiv: 1501.03723 [astro-ph.GA].

McGaugh, S. S. 2012, AJ, 143, 40. https://doi.org/10.1088/0004-6256/143/2/40. arXiv: 1107.2934 [astro-ph.CO].

Milgrom, M. 1983, ApJ, 270, 365. https://doi.org/10.1086/161130.

Milgrom, M. 2010, MNRAS, 403, 886. https://doi.org/10.1111/j.1365-2966.2009.16184.x. arXiv: 0911.5464 [astro-ph.CO].

Mortlock, D. J., et al. 2011, Natur, 474, 616. https://doi.org/10.1038/nature10159. arXiv: 1106.6088 [astro-ph.CO].

Nagesh, S. T., Banik, I., Thies, I., Kroupa, P., Famaey, B., Wittenburg, N., Parziale, R., & Haslbauer, M. 2021, CJP, 99, 607. https://doi.org/10.1139/cjp-2020-0624. arXiv: 2101.11011 [astro-ph.IM].

Oehm, W., & Kroupa, P. 2024, Universe, 10, 143. https://doi.org/10.3390/universe10030143. arXiv: 2403.17999 [astro-ph.GA].

Saglia, R. P., et al. 2016, ApJ, 818, 47. https://doi.org/10.3847/0004-637X/818/1/47. arXiv: 1601.00974 [astro-ph.GA].

Sanders, R. H., & McGaugh, S. S. 2002, ARA&A, 40, 263. https://doi.org/10.1146/annurev.astro.40.060401.093923. arXiv: astro-ph/0204521 [astro-ph].

Thomas, D., Maraston, C., Bender, R., & de Oliveira, C. M. 2005, ApJ, 621, 673. https://doi.org/10.1086/426932. arXiv: astro-ph/0410209 [astro-ph].

Trujillo, I., Ferré-Mateu, A., Balcells, M., Vazdekis, A., & Sánchez-Blázquez, P. 2014, ApJ, 780, L20. https://doi.org/10.1088/2041-8205/780/2/L20. arXiv: 1310.6367 [astro-ph.CO].

van den Bosch, R. C. E., Gebhardt, K., Gültekin, K., van de Ven, G., van derWel, A., & Walsh, J. L. 2012, Natur, 491, 729. https://doi.org/10.1038/nature11592. arXiv: 1211.6429 [astro-ph.CO].

Venemans, B. P., et al. 2013, ApJ, 779, 24. https://doi.org/10.1088/0004-637X/779/1/24. arXiv: 1311.3666 [astro-ph.CO].

Yan, Z., Jerábková, T., & Kroupa, P. 2021, A&A, 655, A19. https://doi.org/10.1051/0004-6361/202140683. arXiv: 2107.[illegible]3388 [astro-ph.GA].

Yldrm, A., van den Bosch, R. C. E., van de Ven, G., Martn-Navarro, I., Walsh, J. L., Husemann, B., Gültekin, K., & Gebhardt, K. 2017, MNRAS, 468, 4216. https://doi.org/10.1093/mnras/stx762. arXiv: 1701.05898 [astro-ph.GA].

People have been building the puzzle pieces of this paper since 1979!

If you want to know more about certain parts of the method, you will probably find more details here.

(Jayde Willingham aka me!)